HORIZON 2020

RESEARCH INFRASTRUCTURES

H2020-INFRAIA-2014-2015

INFRAIA-1-2014-2015 INTEGRATING AND OPENING EXISTING NATIONAL AND REGIONAL RESEARCH INFRASTRUCTURES OF EUROPEAN INTEREST

ENSAR2

EUROPEAN NUCLEAR SCIENCE AND APPLICATION RESEARCH 2

GRANT AGREEMENT NUMBER: 654002

D 13.1 - CREATION AND VALIDATION OF IMPROVED DATA LIBRARIES AND MODELS AND IMPLEMENTATION INTO GEANT4

Version: 1.0
Author: Sylvie LERAY, CEA/IRFU
Date: 24.02.2020

PROJECT AND DELIVERABLE INFORMATION SHEET

ENSAR2 Project Ref. №	654002
Project Title	European Nuclear Science and Application Research 2
Project Web Site	http://www.ensarfp7.eu/
Deliverable ID	D 13.1
Deliverable Nature	Other
Deliverable Level*	PU
Contractual Date of Delivery	28.02.2020
Actual Date of Delivery	26.02.2020
EC Project Officer	René Martins

* The dissemination level are indicated as follows: PU – Public, PP – Restricted to other participants (including the Commission Services), RE – Restricted to a group specified by the consortium (including the Commission Services). CO – Confidential, only for members of the consortium (including the Commission Services).

DOCUMENT CONTROL SHEET

Document	Title: Creation and validation of improved data libraries and models and implementation into GEANT4	
	ID: D 13.1	
	Version: 0.1	
	Software Tool: Microsoft Office Word 2007	
	File: SATNuRSE deliverable D13.1.docx	
Authorship	Written by:	S. Leray
	Contributors:	A. Algora, D. Cano-Ott, J.C. David, E. Mendoza, J.L. Rodriguez-Sánchez, C. Scheidenberger
	Reviewed by:	Muhsin N. Harakeh, KVI Cart
	Approved by:	

DOCUMENT STATUS SHEET

Version	Date	Status	Comments
0.1	23.02.2020	For Internal Review	
1.0	23.02.2020	Final Version	
1.0	26.02.2020	Submitted on EC Participant Portal	
		Final version	

Document Keywords

Keywords	

Disclaimer

This deliverable has been prepared by Work Package 13 (SATNuRSE – Simulations and Analysis Tools for Nuclear Reactions and Structure in Europe) of the Project in accordance with the Consortium Agreement and the Grant Agreement n°654002. It solely reflects the opinion of the parties to such agreements on a collective basis in the context of the Project and to the extent foreseen in such agreements.

Copyright notices

• Introduction

Task 1 of WP13 - SATNuRSE deals with the development of physics models, event generators and their benchmarking and validation. During the previous ENSAR/SiNuRSE project, a platform based on the GEANT4 simulation code was developed and can now be used for experiments foreseen at the ENSAR2 facilities. New event generators and improved physics models relevant in the energy domain of ENSAR2 facilities were implemented in GEANT4 and specific "physics-lists" created. Some members of SiNuRSE have become members of the GEANT4 collaboration, which is very important to make sure that the needs of the nuclear physics community will be taken into consideration. However, further needs to advance the simulation tools were identified, in particular in some domains in which the tools are not reliable enough while essential for the simulation and analysis of experiments realised or foreseen at the ENSAR2 facilities. The objective of this task was therefore to provide, benchmark and validate new or improved physics models and event generators, and implement them in GEANT4. Emphasis was put on domains of nuclear reactions, which have a limited implementation in GEANT4, relevant for facilities of ENSAR2, which were not included in ENSAR, or important for specific key experiments, and the Task was divided into 4 subtasks, as listed below:

- *Subtask 1.1: Improvement and validation of neutron transport models in GEANT4 at neutron energies below 20 MeV (CIEMAT)*

The goal was to extend the capabilities of the GEANT4 toolkit for the simulation of the interaction of neutrons with matter at neutron energies up to 20 MeV. This is of relevance for applications as diverse as the simulation of a neutron detector, an entire particle-physics experiment, a fission or fusion nuclear reactor, a neutron shielding or a hadron-therapy cancer treatment facility.

- *Subtask 1.2: Extension/improvement of the INCL physics models (CEA)*

Two domains of improvements were identified: introducing strange-particle production channels to allow the model to be used for simulations of experiments studying hypernuclei; and improving the predictive power of the model in light-ion induced reactions in the domain of few particle removal channels which are important for both simulation of nuclear structure experiments and some medical applications.

- *Subtask 1.3: Inclusion of modern atomic-interaction routines in GEANT4 (JLU)*

The goal was to implement into GEANT4 the ATIMA (Atomic Interaction with Matter) model developed at Giessen and GSI for the prediction of energy loss and energy-loss straggling of heavy ions up to 1 GeV/u into GEANT4.

- *Subtask 1.4: Electromagnetic cascade model and evaporation of protons and alphas (IFIC)*

The objective was to further develop an event generator for beta-decay by improving the electromagnetic cascade model, and adding the evaporation of other particles like protons and alphas.

All the foreseen developments of the libraries and models have been performed, tested and validated against available experimental data, and the libraries and models implemented into GEANT4 and made available in the last release of the code. In the following, some more details about the subtasks will be presented.

• Subtask 1.1: Improvement and validation of neutron transport models in GEANT4 at neutron energies below 20 MeV (CIEMAT)

The high precision (G4ParticleHP) neutron and charged-particle transport model implemented in the GEANT4 Monte-Carlo code uses nuclear data tables containing the same information as the one available in the ENDF-6 format evaluated data files but written in a different format (G4NDL). The newer releases of the evaluated data libraries have been converted into the GEANT4 format, in particular: JEFF-3.3, JEFF-3.2, ENDF/B-VIII.0, ENDF/B-VII.1, BROND-3.1 and JENDL-4.0u2. The conversion procedure has been done using the latest available version of PREPRO-2017. An exhaustive verification of the converted libraries has been carried out as well. The verification procedure consists of the comparison of Mont-Carlo simulations with the GEANT4 and MCNP6 of identical geometries for each individual isotope present in each evaluated data. Differences between the results obtained were used for assessing the quality of the conversion and for detecting problems/bugs in the converted libraries. An example of this comparison is shown in Fig. 1. It shows the comparison of energy distributions of neutrons produced in one single neutron-induced reaction with ^{235}U with the JEFF-3.3 library: in red the simulation with MCNP6 and in black the simulation with GEANT4.10.3.p02. The new libraries in the G4NDL format will be available for download from the IAEA Nuclear Data Section website dedicated to GEANT4 (https://www-nds.iaea.org/geant4/).

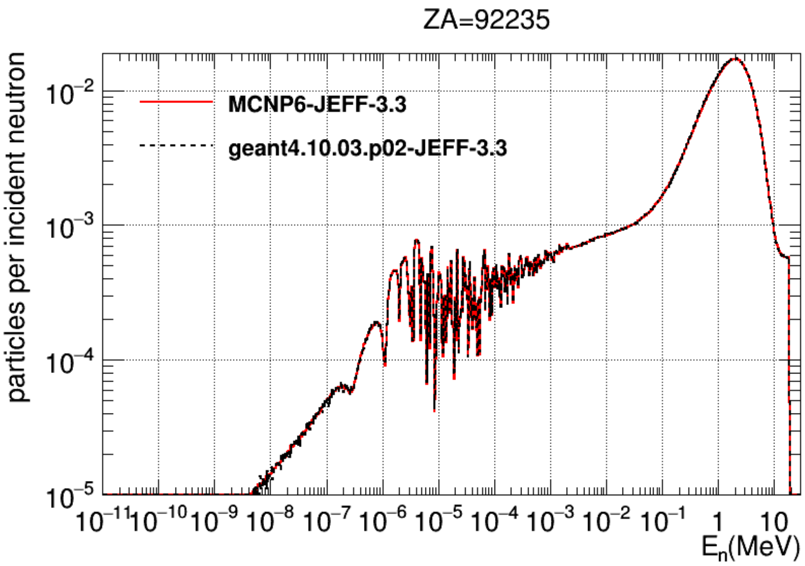

Fig. 1: Comparison of energy distributions of neutrons produced in one single neutron induced reaction with ^{235}U with the JEFF-3.3 library: in red the results with MCNP6 and in black the results with GEANT4.10.3.p02.

• SUBTASK 1.2: EXTENSION/IMPROVEMENT OF THE INCL PHYSICS MODELS (CEA)

The intra-nuclear cascade model, INCL, modelling nucleon and, thanks to ENSAR/SiNuRSE, light-ion induced reactions in the 100 MeV-3 GeV energy domain, has become a reference in the field, and is available in GEANT4. However, further improvements and extensions are still needed in order to allow the code to be universally used in the simulations of experiments or to address specific reaction channels that will be studied in the community of ENSAR2. Two lines of improvement have been identified in SATNuRSE: the introduction of strange-particle production channels for the simulation of experiments on hypernuclei and the improvement of the model in light-ion induced reactions in the domain of few particle-removal channels which are important for both simulation of nuclear structure experiments and medical applications for prediction of the β^+-emitter ^{11}C used in carbon therapy.

- *Introducing strange-particle production channels for the simulation of experiments on hypernuclei*

The production of strange particles (kaons and hyperons) and hypernuclei in light charged-particle induced reactions in the energy range of a few GeV has become a topic of active research at several facilities (e.g., HypHI and PANDA at GSI and/or FAIR (Germany), JLab (USA), and JPARC (Japan)). In this subtask, strange-particle production channels, i.e. kaons and light hyperons, are introduced in INCL in order to allow the model to be used for simulations of experiments studying hypernuclei, in particular in R3B and Super-FRS at the future FAIR facility.

Addition of strange-particle production channels was realised by implementing for each channel: i) the relevant elementary cross sections (production, scattering, and absorption), and ii) the characteristics of all the particles in the associated final states [1]. In a second step, INCL was validated on all the available experimental data on kaon and hyperon production from interaction of light charged particles with nuclei and compared to other models [2].

An example of results is given in Fig. 2 left. The new version of INCL was implemented into the GEANT4 transport code from version 10.4 [3].

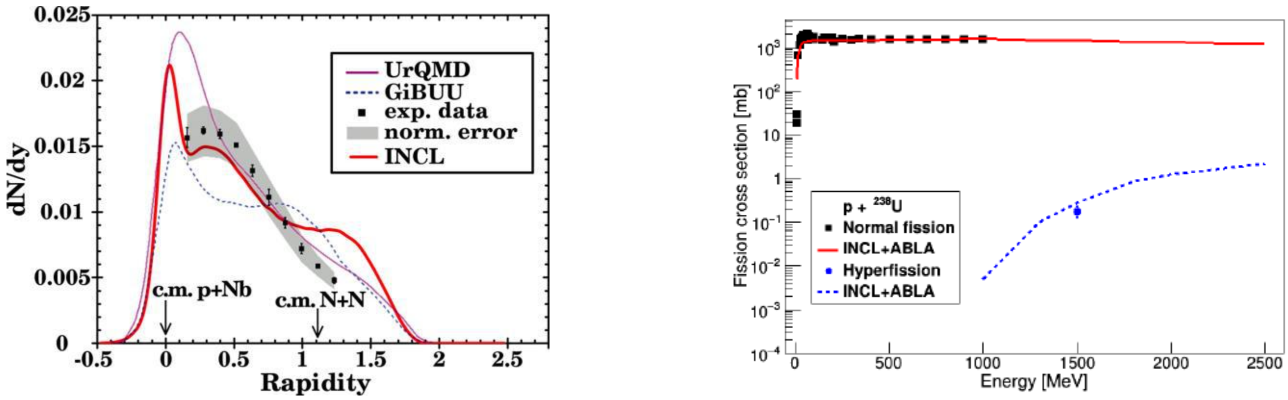

Fig. 2: (left) Λ production yield in p (3.5 GeV) + Nb collisions as a function of rapidity; (right) Fission and hyper-fission cross sections in p + ^{238}U collisions as a function of proton energy.

Production of hypernuclei requires the use of de-excitation model handling hyper-remnants. The ABLA code usually combined to INCL was also upgraded with implementation of the Λ evaporation and treatment of the hyper-fission [4] and after translation into C++ implemented into GEANT4 [5]. Fig. 2 right panel is an illustration of the good results obtained for hyper-fission.

- *improving the predictive power of the model in light-ion induced reactions in the domain of few particle removal channels*

Production of hypernuclei requires the use of de-excitation model handling hyper-remnants. The ABLA code usually combined to INCL was also upgraded with implementation of the Λ evaporation and treatment of the hyper-fission [4] and after translation into C++ implemented into GEANT4 [5]. Figure 2 right panel is an illustration of the good results obtained for hyper-fission.

- *improving the predictive power of the model in light-ion induced reactions in the domain of few particle removal channels*

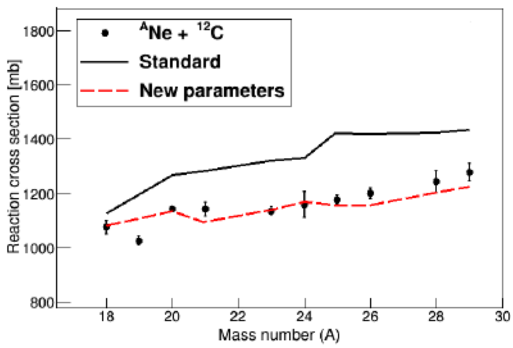

Fig. 3. Total reaction cross sections for different neon isotopes impinging on a carbon target at 950A MeV. Lines correspond to different calculations.

Concerning the few-particles removal channels and light-ions induced reactions and following a work done previously, INCL was improved using Hartree-Fock-Bogoliubov calculations to describe the matter and energy densities in the nuclear surface. These calculations were used to obtain a more realistic description of the radialdensity distributions of protons and neutrons, as well as the excitation-energy anti-correlation at the nuclear surface due to quantum effects and short-range correlations. The new description of the nuclear surface allows to significantly improve the predictions of one-nucleon removal cross sections. It also improves the description of the isotopic cross sections of the heaviest nuclear residues and the total reaction cross sections for nucleon and light-ion induced reactions on nuclei, as shown in Fig. 3 [6].

[1] J. Hirtz et al., Eur. Phys. J. Plus (2018) 133: 436.
[2] J. Hirtz et al., Phys. Rev. C 101, 014608 (2020)
[3] GEANT4 Physics Reference Manual 10.6, p. 333.
[4] J.L. Rodriguez-Sanchez et al., Phys. Rev. C 98, 021602(R) (2018)
[5] GEANT4 Physics Reference Manual 10.6, p. 363.
[6] J.L. Rodriguez-Sanchez et al., Phys. Rev. C 96, 054602 (2017)

• Subtask 1.3: Inclusion of modern atomic-interaction routines in GEANT4 (JLU)

The *ATIMA* (ATomic Interaction with Matter) model developed at GSI [1,2,3] for the prediction of energy loss and energy-loss straggling of ions penetrating matter in a kinetic-energy range from 1 keV/u to 450 GeV/u has been implemented in GEANT4 based on the Fortran version of *ATIMA-1.32*.

In the last two decades, the model has been widely validated for ions using experimental data obtained from experiments carried out at the fragment separator FRS. Basically, the model is based on the Bethe formula but including corrections from the theory developed by Lindhard and Sørensen, which make this model a powerful tool to predict the energy loss and energy-loss straggling of medium-heavy and heavy ions accelerated at relativistic energies.

The implementation in GEANT4 (release version 10.5) was carried out according to the existing GEANT4 structures based on the classes *G4VEmModel* and *G4VEnergyLossProcess*. The source code of *ATIMA* (FORTRAN version 1.32) was translated to *C++* and then included in the GEANT4 toolkit by creating two new classes named *G4AtimaEnergyLossModel* and *G4AtimaFluctuations*, which calculate the energy loss and energy-loss straggling of ions penetrating matter, respectively. For the validation of *ATIMA* model in GEANT4, some tests and extended examples were also created in order to compare the calculations with existing experimental data.

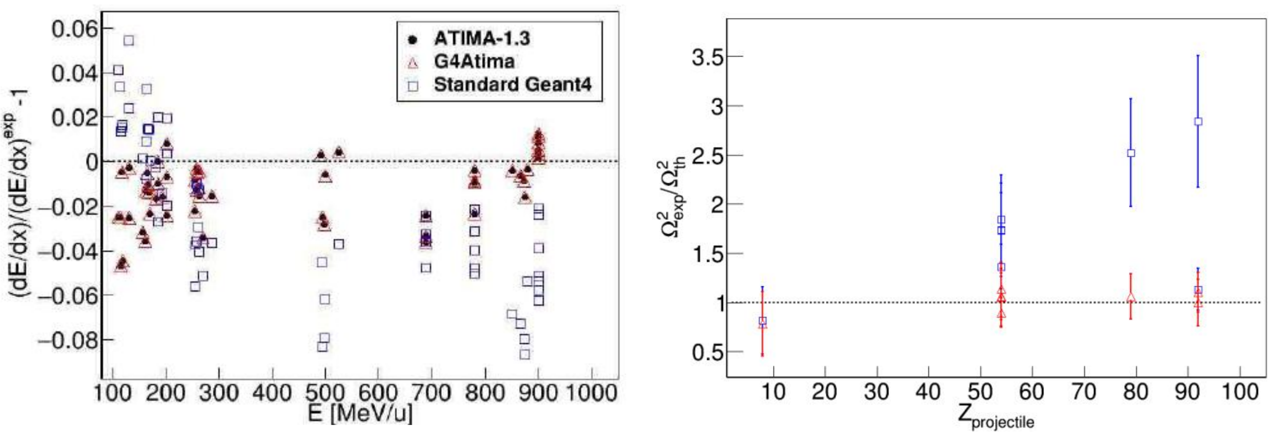

Fig. 4: (Left) Ratio of calculated and measured stopping powers as a function of the projectile kinetic energy for ions from oxygen to uranium. (Right) Ratio of calculated and measured energy-loss straggling as a function of the projectile atomic number.

The results obtained from the benchmark show that the implemented version of *ATIMA* in GEANT4 provides the same energy loss and energy-loss straggling as those from the Fortran version 1.32, as shown in Figs. 1(left) and 1(right), respectively. We also observed that *ATIMA* gives better results than the standard energy-loss model implemented in GEANT4 by default, in particular, when we deal with medium-mass and heavy ions moving at relativistic energies since the Bethe formula based on the first-order Born approximation is not valid anymore and high-order corrections are required to get the exact solution. In addition, a model description was also added to the GEANT4 physics reference manual [4]. Finally, since GEANT4 needs to calculate the energy loss and energy-loss straggling for ions and also for other particles, such as e, μ, protons, etc., *ATIMA* code was included in the GEANT4 physics list library *G4EmStandardPhysicsWVI* of the release version of GEANT4 10.6. This allows for the combination of *ATIMA* with other electromagnetic physics processes modelled by GEANT4.

[1] C. Scheidenberger et al., Phys. Rev. Lett. **73**, 50 (1994).
[2] C. Scheidenberger et al., Phys. Rev. Lett. **77**, 3987 (1996).
[3] H. Weick et al., Phys. Rev. Lett. 85, 2725 (2000).
[4] GEANT4 Physics Reference Manual 10.6, pp. 77-79.

• SUBTASK 1.4: ELECTROMAGNETIC CASCADE MODEL AND EVAPORATION OF PROTONS AND ALPHAS (IFIC)

In the framework of the SiNuRSE project, the IFIC (CSIC-Univ. Valencia) group developed an event generator for beta-decay studies that goes beyond what is presently available in GEANT4, which depends on the evaluated nuclear data available in international databases. In the present SATNuRSE project, this event generator has been further developed and actualised. In this event generator, it is possible to add a continuum of levels that can be populated in beta decay and those added levels can de-excite by the emission of electromagnetic cascades to discrete known levels and also to the levels added in the continuum. The user can decide at which excitation the continuum of levels begins. The levels are generated based on level-density function parameterisations. The electromagnetic de-excitation is based on gamma strength functions of type E1, M1 and E2. The parameters necessary for the level-density functions and for the gamma strength functions are taken from the RIPL-3 database [1]. This database is also useful for deciding up to which excitation energy the level scheme populated in the beta decay can be considered complete. The created tools can also be used for generating photon evaporation tables for GEANT4, using the information available in evaluated nuclear data bases (accepted levels and electromagnetic de-excitation branches) and complemented with information available from RIPL-3 as mentioned before (using levels and branches deduced from level-density functions and gamma-strength functions of type E1 M1 and E2).

The developed tools have been successfully used in the analysis of the beta decay of ^{186}Hg measured with the total absorption technique at ISOLDE [2] and have been presented in a GEANT4 workshop organised by the SATNuRSE task 4 [3]. In addition, in the event generator beta-delayed *n*, *p*, and alpha emission has been implemented using optical parameters extracted from the TALYS code. For the emission of beta-delayed neutrons, the use of a square potential is also possible.

[1] R. Capote et al., Nuclear Data Sheets 110, 3107 (2009); https://www-nds.iaea.org/RIPL-3/
[2] E. Ganioglu, A. Algora et al., in preparation
[3] A. Algora, D. Jordan, E. Ganioglu, E. Nácher, J. L. Tain (presented by E. Nácher), *Extending GEANT4 "Radioactive Decay" for Complex Total Absorption Analysis Cases,* ENSAR2 workshop: GEANT4 in nuclear physics, Madrid, April 24-26, 2019

ANNEX 1

Sub-Task 13.1:

Improvement and validation of neutron transport models in GEANT4 at neutron energies below 20 MeV

E. Mendoza and D. Cano-Ott

Centro de Investigaciones Energéticas, Medioambientales y Tecnológicas (CIEMAT), Madrid, Spain

ABSTRACT

The Monte Carlo simulation of the interaction of neutrons with matter relies on evaluated nuclear data libraries and models. The evaluated libraries are compilations of measured physical parameters (such as cross sections) combined with predictions of nuclear model calculations which have been adjusted to reproduce the experimental data. The results obtained from the simulations depend largely on the accuracy of the underlying nuclear data used, and thus it is important to have access to the nuclear data libraries available, either of general use or compiled for specific applications, and to perform exhaustive validations which cover the wide scope of application of the simulation code. In this paper we describe the work performed in order to extend the capabilities of the GEANT4 toolkit for the simulation of the interaction of neutrons with matter at neutron energies up to 20 MeV and a first verification of the results obtained. Such a work is of relevance for applications as diverse as the simulation of a neutron detector, an entire particle physics experiment, a fission or fusion nuclear reactor, a neutron shielding or a hadron therapy cancer treatment facility.

We have converted the newer releases of the evaluated data libraries into the Geant4 format and implemented the necessary secondary production models as defined by the libraries: JEFF-3.3, JEFF-3.2, ENDF/B-VIII.0, ENDF/B-VII.1, BROND-3.1 and JENDL-4.0u2. We have performed as well an exhaustive verification of the converted libraries. The verification consists in the comparison of Monte Carlo simulations with the Geant4 and MCNP6 of identical geometries for each individual isotope present in each evaluated data. The nuclear data have been disseminated at the IAEA Nuclear Data Section website dedicated to GEANT4 (https://www-nds.iaea.org/geant4/).

1. INTRODUCTION

The so-called High Precision neutron physics model implemented in the Geant4 [1] simulation package allows simulating the transport of neutrons with energies up to 20 MeV. It relies on the G4NDL cross section libraries, prepared by the Geant4 collaboration from evaluated cross section files, originally written in ENDF-6 format [2], and distributed freely together with the code. In order to have more flexibility when performing Monte Carlo simulations we developed a tool for transforming any ENDF-6 format evaluated neutron cross section library into the G4NDL format [3]. In 2012, eight different releases of the ENDF, JEFF, JENDL, CENDL and BROND libraries were translated into the G4NDL format and distributed by the IAEA Nuclear Data Services [4]. Since then, new releases of these libraries have appeared. For this reason, we have updated the list of G4NDL distributed libraries with six new releases, which are: JEFF-3.3 [5], JEFF-3.2 [6], ENDF/B-VIII.0 [7], ENDF/B-VII.1 [8], BROND-3.1 [9] and JENDL-4.0u [9] (version 2016/1/6 [11]).

In this report we provide some information concerning the conversion process of these six new releases into the G4NDL format. In addition, we present a comparison between results obtained with Geant4 and MCNP6 when using these libraries.

2. PRODUCTION OF THE LIBRARIES

The new libraries were produced in a similar way as the older releases, but using PREPRO-2017 [12] instead of PREPRO-2010.

The cross sections used in Geant4 files have to appear in a linear interpolative form. For this reason, it was necessary to pre-process the ENDF-6 format libraries, since the cross section data are given in files MF=2 (resonance parameters) and MF=3 (data points). It was necessary to transform the MF=3 file (which can be expressed also in log-log or linear-log interpolation laws) into a linear-linear interpolative form, and then add the contribution of file MF=2 to file MF=3.

The procedure was performed with the PREPRO software package, a collection of public and standard computing codes distributed by the IAEA which allow converting the ENDF-6 libraries into a form required by many applications. The production scheme used is as follows:

1. First the LINEAR programme was applied, in order to change the cross-section data points in file MF=3 into linear-linear interpolation form. The allowable error was set to 0.1%.
2. Then the RECENT programme was applied, in order to convert the resonance contribution into cross section data points. The allowable error was set to 0.1%.
3. Then the LINEAR programme was applied again, in order to reduce the number of cross section points in file MF=3. The allowable error was set to 1%, since an error smaller than 1% leads to an excessively large number of points (>500.000) for some cross sections.
4. Then the FIXUP programme was applied. It reads the ENDF-6 file and performs some format corrections, if needed.
5. Finally the DICTIN programme was applied, in order to update the section index in MF=1, MT=451.

Once the ENDF-6 data file is processed with PREPRO, the result (still in ENDF-6 format) is translated with a specific programme developed by the authors into the G4NDL data format.

Some specific issues which appeared when creating the libraries are the following:

a) JEFF-3.3:
   - ^{9}Be: secondary neutrons of reaction (*n*,2*n*) are described with reaction types MT=875 to MT=891 instead of MT=16. Geant4 is not able to read such data in this format, therefore reaction (*n*,2*n*) has been replaced with the (*n*,2*n*) appearing in JEFF-3.0, which uses MT=16.
   - ^{232}Th, ^{231,233}Pa: MF=6 data (product energy-angle distributions) for MT=18 (fission) has been converted to MF=4,5,12,14,15 with the PREPRO SIXPAK programme before the translation into the G4NDL format, since Geant4 is not able to read such data in MF=6 format.

b) JEFF-3.2:

- ^{9}Be: secondary neutrons of reaction (*n*,2*n*) are described with reaction types MT=875 to MT=891 instead of MT=16. Geant4 is not able to read such data in this format, therefore reaction (*n*,2*n*) has been replaced with the (*n*,2*n*) appearing in JEFF-3.0, which uses MT=16.
- ^{46,47,48,49,50}Ti: there is a bug in the ENDF-6 format library in the gamma ray emission after neutron capture. The bug has been corrected by editing the file "by hand".
- ^{232}Th, ^{231,233}Pa: MF=6 data (product energy-angle distributions) for MT=18 (fission) has been converted to MF=4,5,12,14,15 with the PREPRO SIXPAK programme before the translation into the G4NDL format, since Geant4 is not able to read such data in MF=6 format.

c) ENDF/B-VIII.0:
- ^{232}Th, ^{231,233}Pa: MF=6 data (product energy-angle distributions) for MT=18 (fission) has been converted to MF=4,5,12,14,15 with the PREPRO SIXPAK programme before the translation into the G4NDL format, since Geant4 is not able to read such data in MF=6 format.

d) ENDF/B-VII.1:
- ^{232}Th, ^{231,233}Pa: MF=6 data (product energy-angle distributions) for MT=18 (fission) has been converted to MF=4,5,12,14,15 with the PREPRO SIXPAK programme before the translation into the G4NDL format, since Geant4 is not able to read such data in MF=6 format.
- ^{241,243}Am: MF=5, MT=18 (energy distribution of fission neutrons) are described with LF=12 (energy dependent Madland-Nix spectrum). Geant4 has some problems with this LF=12 energy distribution law so the data were converted to LF=1 (arbitrary tabulated function) with the PREPRO SPECTRA programme before the translation into the G4NDL format.

e) BROND-3.1:
- ^{240}Pu: MF=6 data (product energy-angle distributions) for MT=18 (fission) has been converted to MF=4,5,12,14,15 with the PREPRO SIXPAK programme before the translation into the G4NDL format, since Geant4 is not able to read such data in MF=6 format.
- ^{241,243}Am, ^{243,244}Cm: MF=5, MT=18 (energy distribution of fission neutrons) are described with LF=12 (energy dependent Madland-Nix spectrum). Geant4 have some problems with this LF=12 energy distribution law so the data was converted to LF=1 (arbitrary tabulated function) with the PREPRO SPECTRA programme before the translation into the G4NDL format.

f) JENDL-4.0u:
- No issue to be mentioned.

3. COMPARISON WITH MCNP6

We have verified the integrity of the new G4NDL libraries by performing identical simulations with Geant4 and MCNP6. These simulations are the ones described in [3] (Section III.B.1). The geometry of the simulations consists in a 2 m long cylinder with a radius of 1 μm made of an isotopically pure material with density 1 g/cm^3. The source consists of neutrons isolethargically distributed with energies ranging from 10^{-10} to 19 MeV impinging on the centre of the cylinder along its symmetry axis. The small cylinder radius allows to simulate one neutron interaction per event and the secondary particles to leave the cylinder without suffering almost any interaction. The energies and angles of the secondary neutrons, gamma-rays, protons, deuterons, tritons, ^{3}He and alphas are stored in 2-dimensional histograms, one per secondary particle type. The results obtained with these simulations depend on all the partial cross sections and probability distributions present in the libraries.

Two simulations were performed for each isotope present in each of the six converted libraries: one using Geant4 (version geant4.10.04.p01), with 10^7 source neutrons, and the other using MCNP6, with 10^8 source neutrons. In Geant4 the environmental variable "G4NEUTRONHP_DO_NOT_ADJUST_FINAL_STATE" was defined, and in MCNP6 the unresolved resonance range probability table treatment was turned off. These two physics options make the results obtained more comparable with both codes.

An example of the obtained results is presented in Fig. 1, where we present the projection in energies of the 2-dimensional histogram of the secondary neutrons for ^{16}O as the cylinder material (ZA=1000·Z+A=8016). In both Geant4 and MCNP6 simulations the JEFF-3.3 library was used. In this case both results are in good agreement above 1 eV. Discrepancies below 1 eV are due to differences in the thermal treatment of the codes. A similar discrepancy below 1 eV is obtained for all nuclei without large absorption cross sections at low neutron energies, with the exception of ^{1}H where the results obtained with both codes are in agreement.

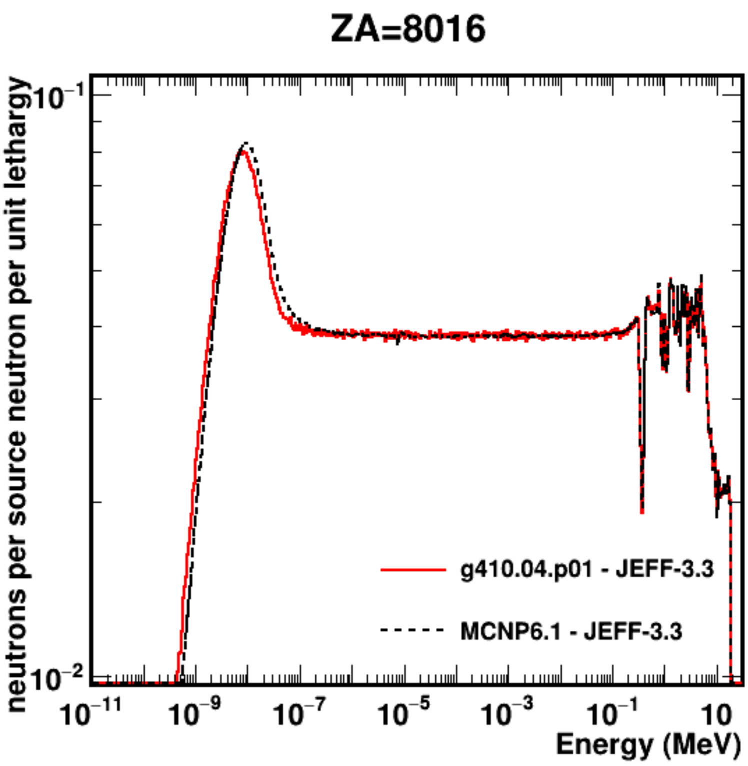

FIG. 1. Energy distributions integrated over all angles of the secondary neutrons obtained with Geant4 and with MCNP6 for ^{16}O (see the text for more details).

The systematic comparison between the results obtained with both codes allow to check the integrity of the G4NDL converted data libraries (the specific issues reported in Section 0 were found after performing these comparisons). It also allows to detect bugs in the Geant4 code. This can be done (and has been done in the past [3]) by identifying in which nuclei there are discrepancies. Then, the format defining the relevant probability distributions for those nuclei is defined. This allows to locate the parts of the code which should be corrected, which are the parts which manage these probability distributions.

In order to quantify the differences in the neutron transport obtained with both codes we have systematically compared the energy distributions integrated over all angles of the secondary neutrons obtained with Geant4 and with MCNP6, i.e. the projection in energies of the 2-dimensional histogram of the secondary neutrons (Fig. 1). This comparison has been performed by computing three different variables for each nuclei of each library, d_1, d_2 and χ_v^2, defined as:

$$d_1 = \frac{1}{N} \sum_{E_i > 1\ eV} \frac{|x_i^G - x_i^M|}{\frac{1}{2}(x_i^G + x_i^M)}$$

$$d_2 = \frac{1}{N} \sum_{E_i > 1\ eV, \sigma_i < 1\%} \frac{|x_i^G - x_i^M|}{\frac{1}{2}(x_i^G + x_i^M)}$$

$$\chi_v^2 = \frac{1}{N} \sum_{E_i > 1\ eV} \left(\frac{x_i^G - x_i^M}{\sigma_i}\right)^2$$

where x_i^G and x_i^M are, respectively, the contents of the i bin of the Geant4 and MCNP6 histograms; σ_i are the uncertainty of the i bin due to counting statistics, computed as the square root of the quadratic sum of the uncertainties in x_i^G and x_i^M; and N is the number of bins considered in the sum. All three variables have been computed for energies above 1 eV, due to the different thermal treatment of the codes mentioned above. d_1 is the average difference between the bin contents. Part of this difference is due to counting statistics, so we defined d_2 same as d_1 but only bins with uncertainties below 1% are considered. χ_v^2 is the reduced chi-squared between both results, and measures the difference between the results in terms of their uncertainties. Note then that a large value of χ_v^2 does not mean a large difference in the obtained results, but a large difference compared with the achieved uncertainties due to counting statistics, which can be reduced by simulating more source neutrons. Indeed, the χ_v^2 is expected to diverge to infinity as the number of source neutrons used in the simulation increases, since the results obtained with both codes are not expected to be exactly the same.

The values of d_1, d_2 and χ_v^2 are presented in histograms in 0Figs. 5-10 for all the isotopes (but the isomers) present in each of the six transformed libraries. The results are presented in both linear and logarithmic Y axis. Values of d_1 and d_2 greater than 5% have been set to 5%, and χ_v^2 values greater than 5 have been set to 5, for convenience in the representation.

One important note is that in the case of the JENDL library we did not use exactly the same release in MCNP6 (JENDL-4.0, the first release, in 2010) than in Geant4 (JENDL-4.0u version 2016, an updated release). The changes in JENDL-4.0u with respect to JENDL-4.0 are listed in [13].

The results of the simulations performed with both codes deviate less than a few percent in most of the cases. Results with d_1 or d_2 larger than 5% are listed in Table 1. The origin of the discrepancies in ^{135}Cs in JEFF-3.3 has not been identified but the problem seems to be in the MCNP6 result. The results obtained for ^{7}Be in ENDF/B-VII.1 and ^{233}Pa in BROND-3.1 differ significantly, but we did not identify the reason. ^{231}Th in BROND-3.1 appear with a negative elastic cross section at low neutron energies. The differences in the two JENDL isotopes are due to updates in the JENDL library.

TABLE 1. NUCLEI WITH d_1 OR d_2 LARGER THAN 5%, TOGETHER WITH d_1, d_2 AND χ_υ^2.

ZA - LIB	d_1	d_2	χ_υ^2
55135 – JEFF-3.3	4.04	6.98	122
4007 – ENDF/B-VII.1	5.99	-	33.2
90231 – BROND-3.1	14.4	2.63	20.8
91233 – BROND-3.1	6.96	14.0	134
5010 – JENDL-4.0u	8.69	-	4.58
63156 – JENDL-4.0u	24.1	0.71	626

Other nuclei with smaller but significant discrepancies (isotopes with $\chi_\upsilon^2 > 2$ and $d_2 > 1.5\%$) are listed in Table 3 to Table 8. These two conditions in χ_υ^2 and d_2 are arbitrary, but we have adopted them to list the discrepant nuclei after testing various types of conditions. The amount and the fraction of isotopes which fulfil these conditions are given in Table 2.

TABLE 2. NUMBER OF ISOTOPES OF EACH OF THE SIX CONVERTED LIBRARIES, TOGETHER WITH THE AMOUNT OF ISOTOPES WITH $\chi_\upsilon^2 > 2$ AND $d_2 > 1.5\%$. THE NUMBER OF ISOTOPES TESTED IS NOT THE SAME AS THE TOTAL NUMBER OF ISOTOPES IN EACH LIBRARY SINCE WE DIDN'T TEST THE ISOMERS.

Library	Total number of isotopes	Number of isotopes tested	Number of isotopes with $\chi_\upsilon^2 > 2$ and $d_2 > 1.5\%$	Fraction of isotopes with $\chi_\upsilon^2 > 2$ and $d_2 > 1.5\%$	Number of isotopes with $\chi_\upsilon^2 > 2$	Fraction of isotopes with $\chi_\upsilon^2 > 2$
JEFF-3.3	562	546	34	6%	51	9%
JEFF-3.2	472	460	52	11%	78	17%
ENDF/B-VIII.0	556	533	84	16%	114	21%
ENDF/B-VII.1	423	411	90	22%	120	29%
BROND-3.1	372	361	64	18%	78	22%
JENDL-4.0u	406	398	58	15%	87	22%

An example of a good agreement between both simulated results has been presented in 0Fig. 1. In that case $d_1 = 0.9\%$, $d_2 = 0.8\%$ and $\chi_\upsilon^2 = 1.4$. Two examples with $\chi_\upsilon^2 > 2$ and $d_2 > 1.5\%$ are shown in Fig. 2 (^{138}Ba) and Fig. 3 (^{245}Cm). The discrepancies found for the actinides listed in Table 3 to Table 8 are similar to the one presented in Fig. 3 for ^{245}Cm. This suggests that there could be some bug in Geant4 affecting the energy of the fission neutrons. These discrepancies are not found in all the fission nuclei. As an example, the results obtained for ^{235}U with JEFF-3.3 are provided in 0Fig. 4.

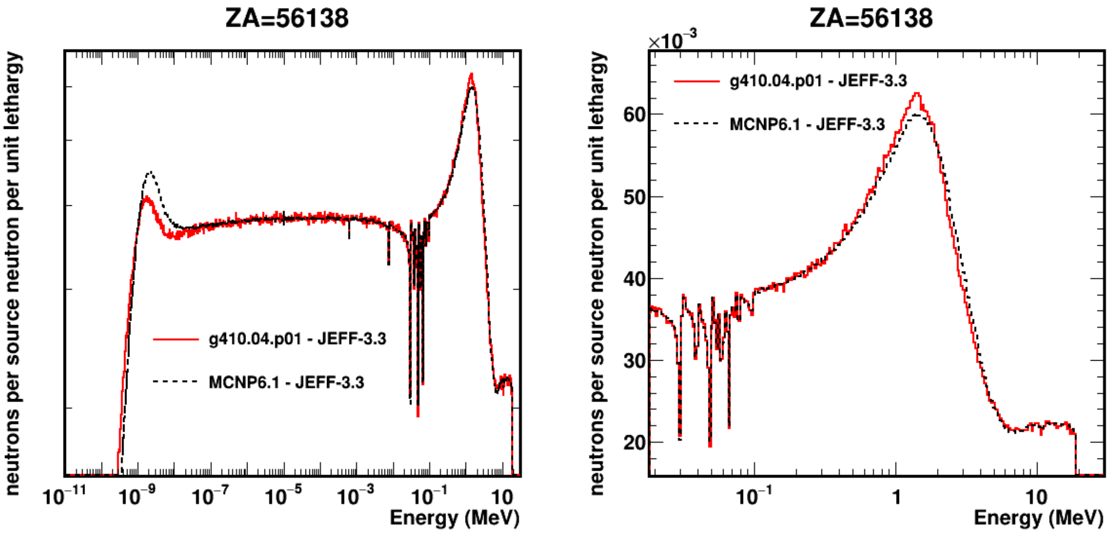

FIG. 2. Energy distributions integrated over all angles of the secondary neutrons obtained with Geant4 and with MCNP6 using JEFF-3.3 for ^{138}Ba (see the text for more details). The right panel is a zoom of the left panel. In this case, $d_1 = 1.13\%$, $d_2 = 1.64\%$ and $\chi^2_\upsilon = 2.9$.

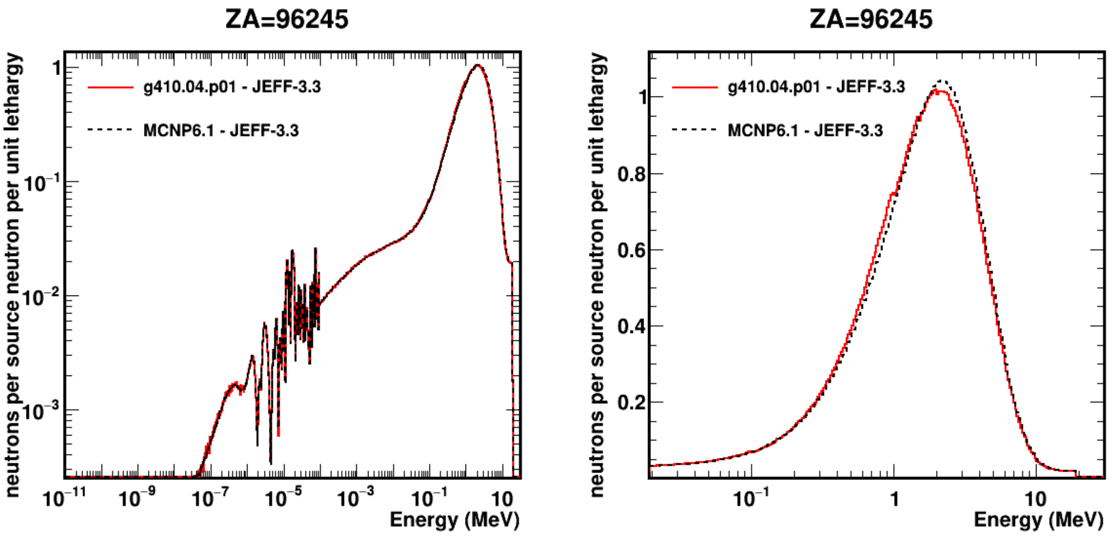

FIG. 3. Energy distributions integrated over all angles of the secondary neutrons obtained with Geant4 and with MCNP6 using JEFF-3.3 for ^{245}Cm (see the text for more details). The right panel is a zoom of the left panel. In this case, $d_1 = 2.81\%$, $d_2 = 3.74\%$ and $\chi^2_\upsilon = 72$.

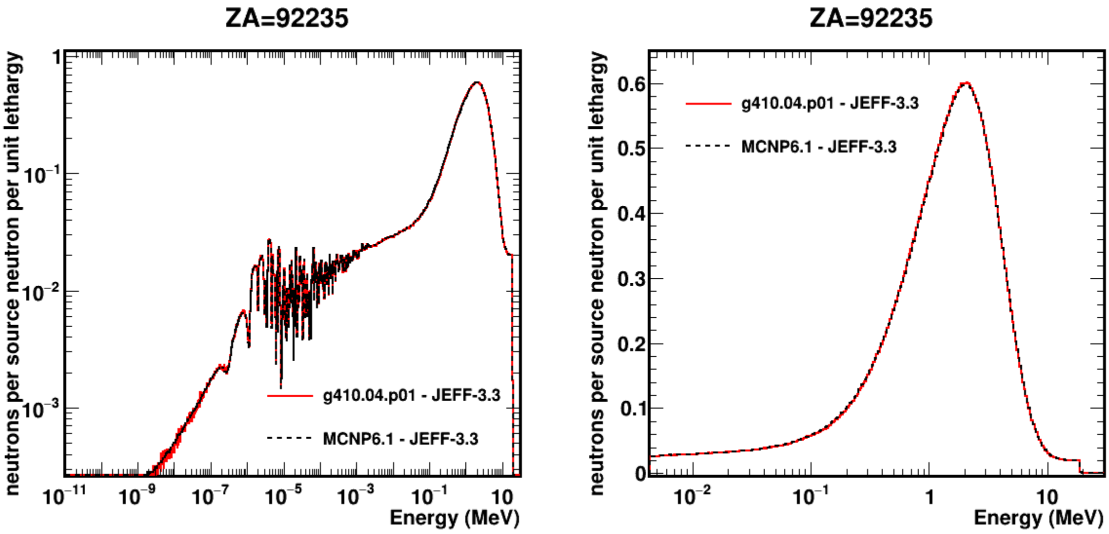

FIG. 4. Energy distributions integrated over all angles of the secondary neutrons obtained with Geant4 and with MCNP6 using JEFF-3.3 for ^{235}U (see the text for more details). The right panel is a zoom of the left panel. In this case, $d_1 = 1.80\%$, $d_2 = 1.13\%$ *and* $\chi_v^2 = 3.2$.

The full set of plots of the energy distributions integrated over all angles of the secondary neutrons obtained with both codes (i.e. similar to the ones presented in Figs 1-4) are available in the IAEA Nuclear Data Services [4] together with the libraries. In addition, similar plots, but with the energy distributions of secondary protons, deuterons, tritons, ^{3}He, alphas and γ-rays, are also provided. There is one plot for each of the mentioned secondary particles, for each nucleus (but the isomers) present in the six distributed libraries.

In the case of secondary particles different from neutrons, we didn't make a systematic comparison between Geant4 and MCNP6 with d_1, d_2 and χ_v^2 similar to the one performed with neutrons and described in this report. This is because in this case the comparison is not so straightforward. In the ENDF-6 format libraries the energy and angles of the secondary neutrons are always provided, but for the rest of the secondary particles these distributions are sometimes omitted. Where they are omitted, Geant4 will use a model to generate them whereas MCNP6 will not produce them.

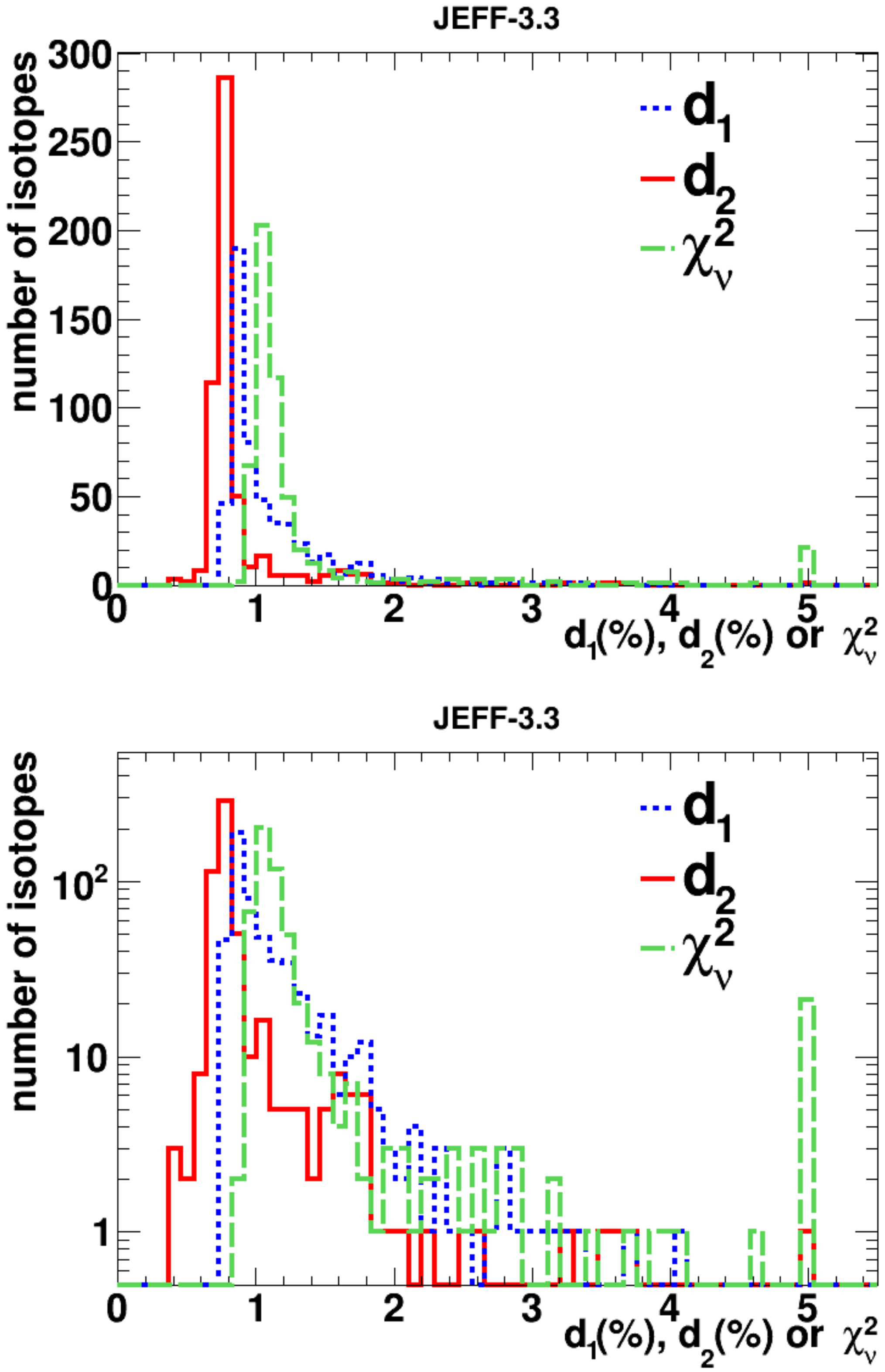

FIG. 5. Number of isotopes with different values of d_1, d_2 and χ^2_υ obtained with JEFF-3.3.

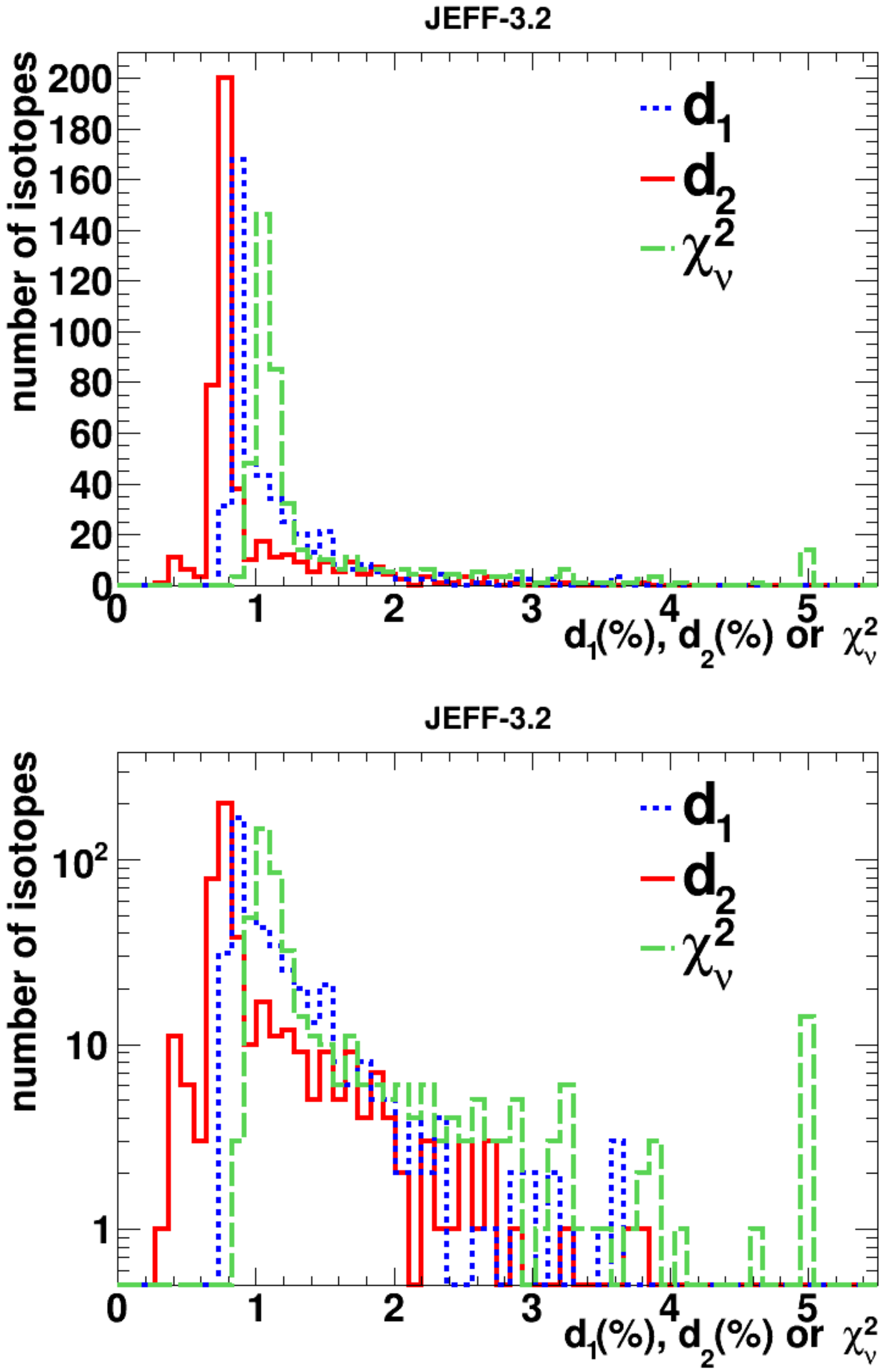

FIG. 6. Number of isotopes with different values of d_1, d_2 and χ_v^2 obtained with JEFF-3.2.

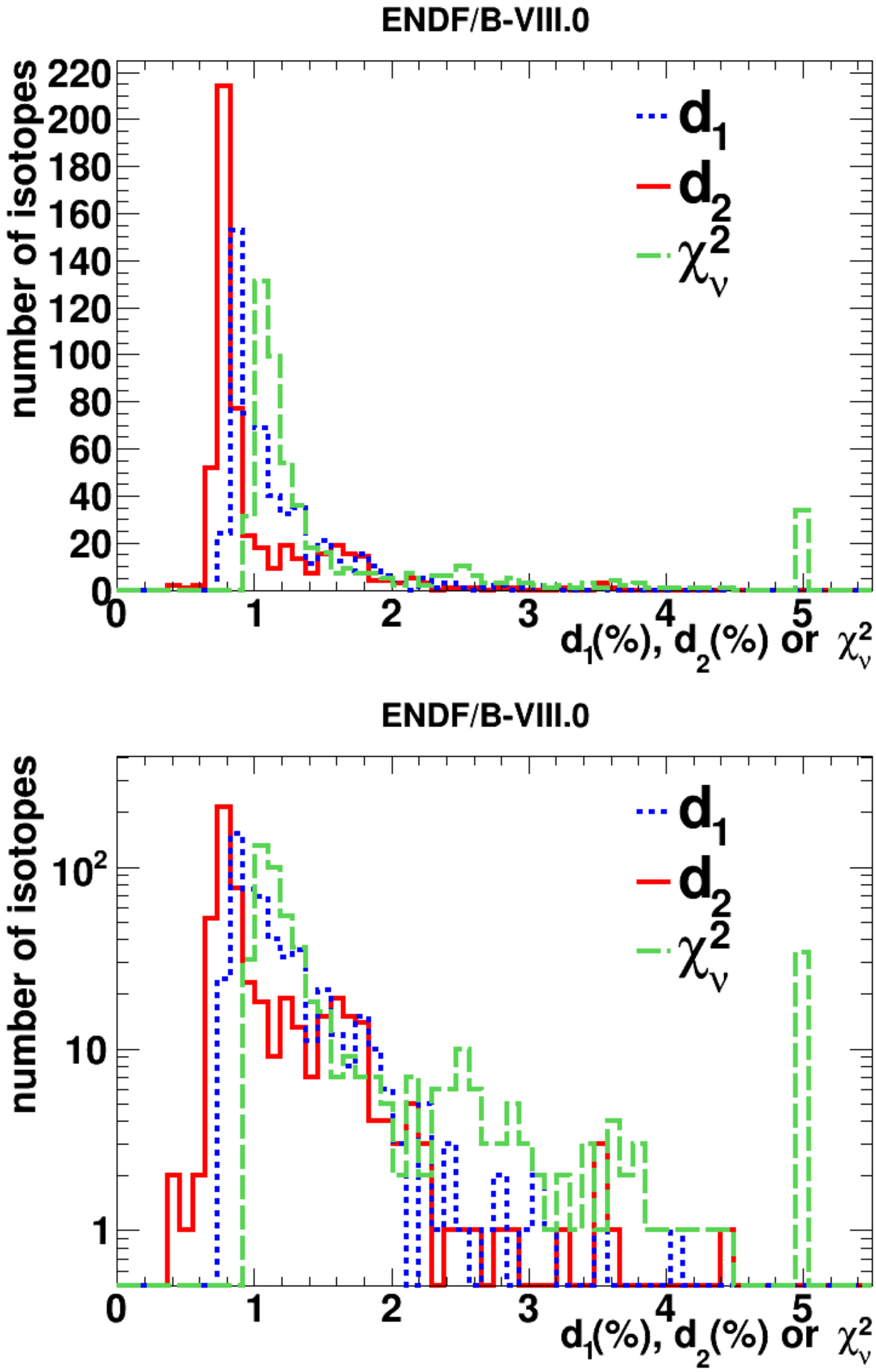

FIG. 7. Number of isotopes with different values of d_1, d_2 and χ_v^2 obtained with ENDF/B-VIII.0.

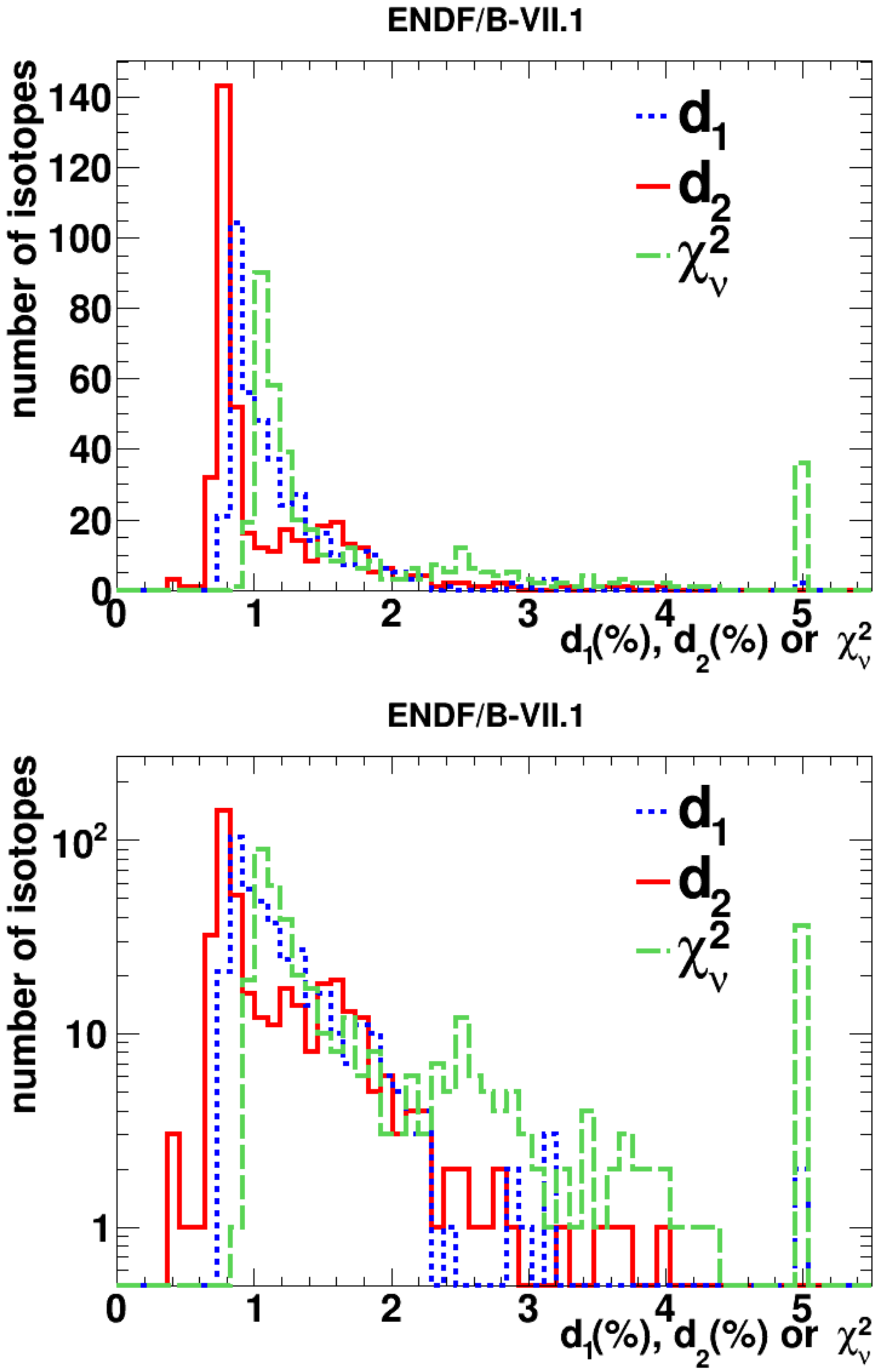

FIG.8. Number of isotopes with different values of d_1, d_2 and χ_υ^2 obtained with ENDF/B-VII.1.

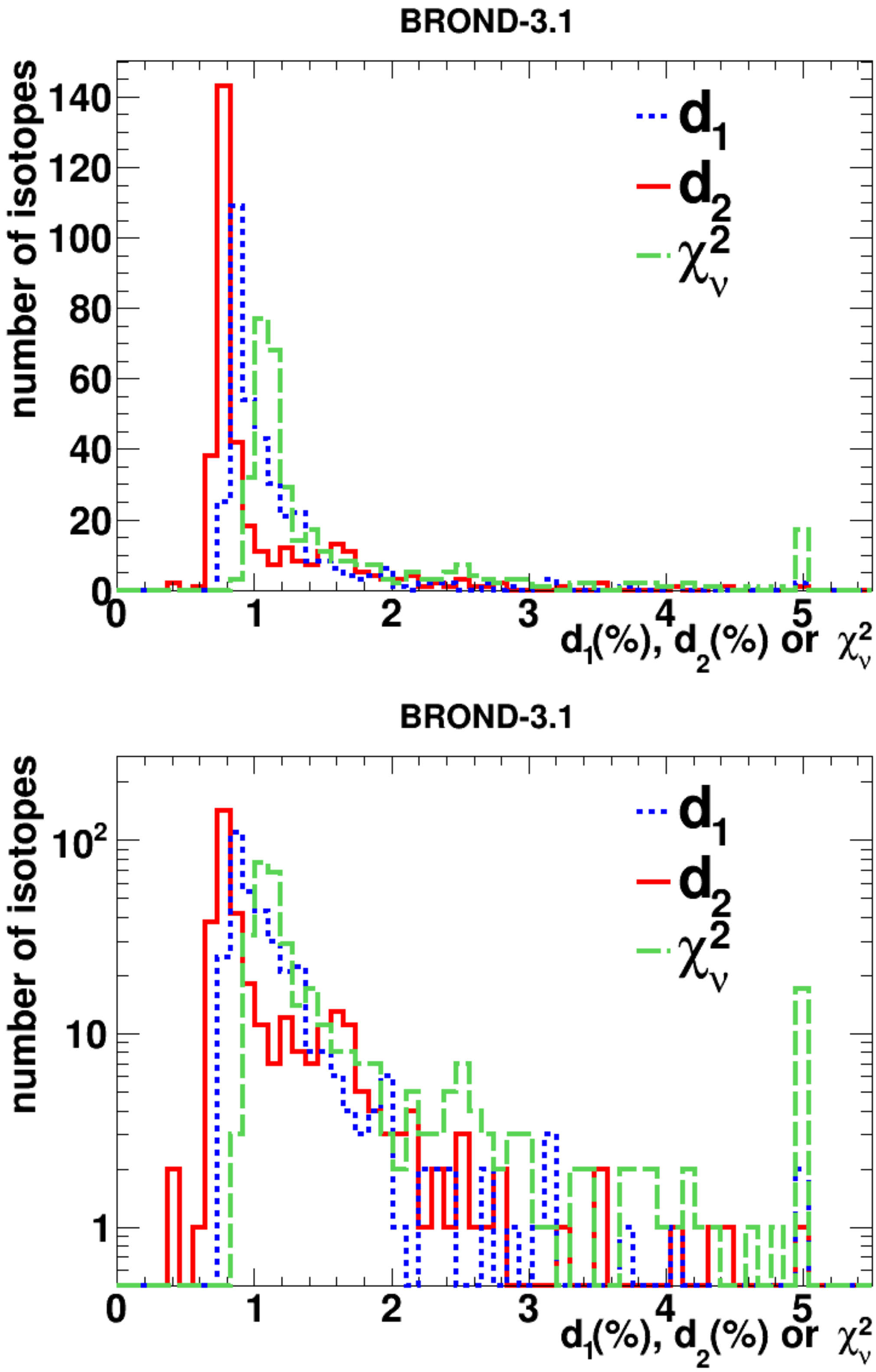

FIG. 9. Number of isotopes with different values of d_1, d_2 and χ^2_υ obtained with BROND-3.1.

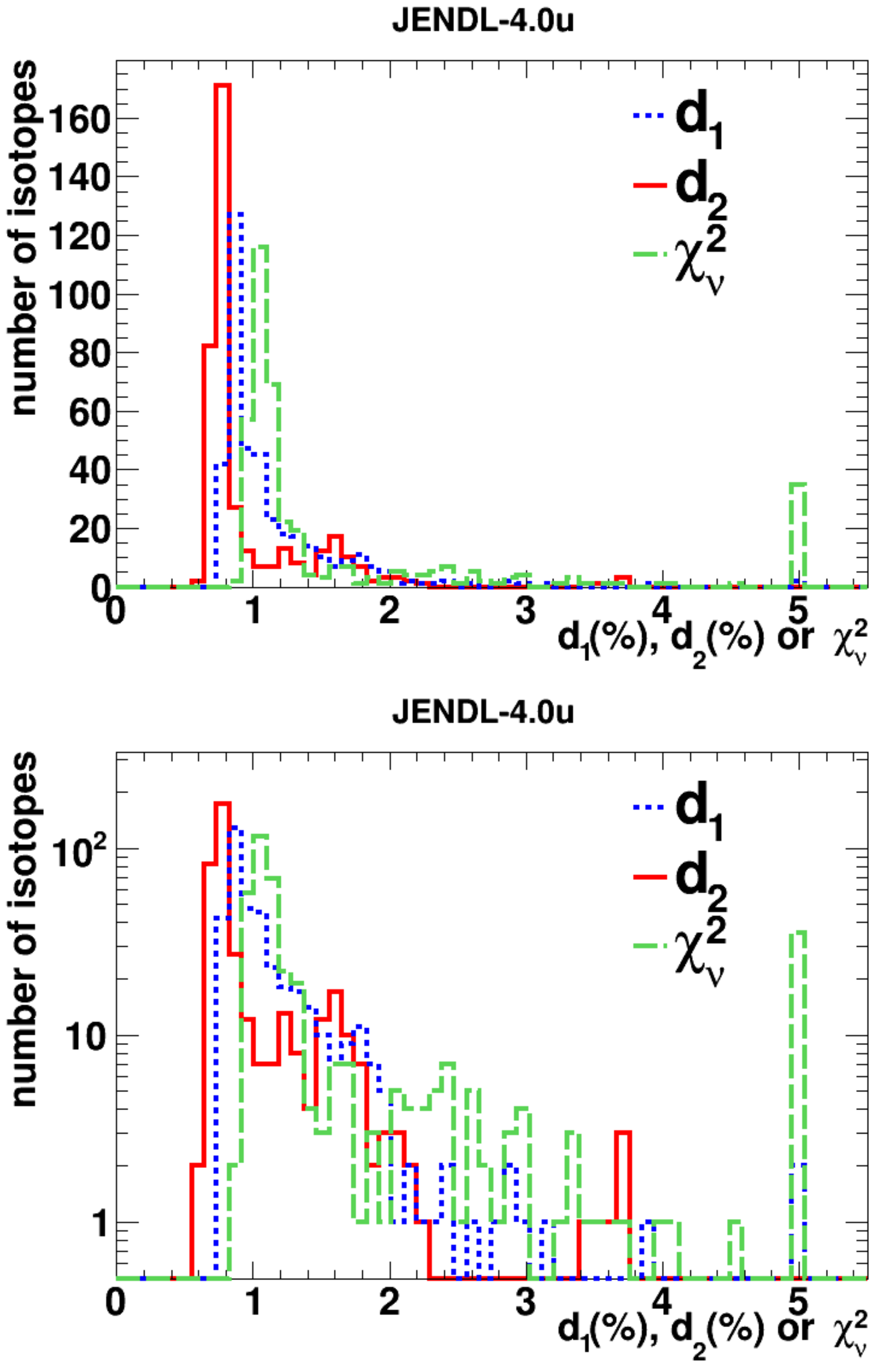

FIG. 10. Number of isotopes with different values of d_1, d_2 and χ^2_υ obtained with JENDL-4.0u.

TABLE 3. Nuclei from JEFF-3.3 with $\chi_v^2 > 2$ and $d_2 > 1.5$, together with d_1, d_2 and χ_v^2.

ZA	d_1(%)	d_2(%)	χ_v^2
46107	1.22	1.64	2.41
53131	1.30	1.81	2.80
55135	4.04	6.98	122
56130	1.16	1.80	2.05
56132	1.18	1.89	2.39
56134	1.14	1.70	2.23
56135	1.24	1.95	2.62
56136	1.14	1.69	2.60
56137	1.10	1.75	2.34
56138	1.13	1.64	2.88
59143	1.26	1.61	3.13
61147	1.55	2.48	3.94
61148	2.36	3.22	6.18
63151	2.18	2.63	3.68
63154	1.97	1.58	2.19
91231	2.00	2.26	4.11
91232	1.76	1.56	5.94
92232	1.49	1.51	5.28
92233	2.77	3.56	51.7
93236	1.95	1.56	7.32
94236	1.90	1.76	9.18
94241	1.73	1.55	7.29
95242	2.18	1.79	18.3
95244	1.73	1.58	6.72
96241	1.83	1.73	10.3
96242	1.62	2.07	7.55
96243	3.29	3.67	64.5
96245	2.81	3.74	72.4
96247	1.87	1.62	8.85
96249	1.72	1.68	8.92
98249	1.74	1.67	9.87
98253	1.87	1.59	9.27
99254	2.29	1.73	12.1
100255	2.17	1.76	12.8

TABLE 4. Nuclei from JEFF-3.2 with $\chi_v^2 > 2$ and $d_2 > 1.5$, together with d_1, d_2 and χ_v^2.

ZA	d_1(%)	d_2(%)	χ_v^2
41094	1.30	1.74	2.85
42099	1.28	1.73	2.59
45105	1.36	1.50	3.28
46107	1.28	1.82	2.63
49113	1.45	1.81	2.56
49115	1.49	1.85	2.68
50117	1.36	2.40	3.86
50119	1.08	1.63	2.29
53131	1.31	1.88	2.77
54128	1.12	1.52	2.27
54129	1.25	1.74	2.31
54133	1.29	1.53	2.14
55135	1.27	1.97	3.20
55137	1.22	1.73	3.22
56130	1.22	1.85	2.33
56132	1.18	1.89	2.42

56134	1.10	1.62	2.20
56135	1.20	1.92	2.59
56136	1.13	1.70	2.40
56137	1.11	1.72	2.42
56138	1.25	2.00	3.38
58144	1.17	1.97	2.89
59143	1.20	1.61	2.84
60148	1.58	1.68	3.08
61147	1.55	2.48	3.94
61148	2.36	3.22	6.18
61149	1.96	2.27	3.57
62149	1.90	2.34	3.28
63151	2.17	2.63	3.68
63152	3.60	2.71	17.7
63153	1.83	1.65	2.00
63156	1.52	1.98	3.13
65159	1.58	2.54	3.80
72174	1.52	2.26	2.86
72176	1.32	1.89	2.67
72177	1.79	2.75	3.80
72178	1.66	2.05	3.18
72179	1.50	2.69	3.87
73182	1.46	1.62	2.63
80198	1.25	1.78	3.26
80199	1.60	2.88	5.86
80201	1.45	2.56	5.03
91231	1.69	2.24	4.10
91232	1.76	1.55	5.85
95242	2.25	1.86	18.2
96241	1.81	1.72	10.2
96242	1.43	2.05	7.59
96243	3.40	3.74	65.0
96245	2.94	3.79	72.7
96247	1.86	1.63	8.92
96249	1.73	1.68	8.90
98253	1.87	1.56	9.15

TABLE 5. Nuclei from ENDF/B-VIII.0 with $\chi_v^2 > 2$ and $d_2 > 1.5$, together with d_1, d_2 and χ_v^2.

ZA	d_1(%)	d_2(%)	χ_v^2
8018	4.08	4.47	94.7
35081	1.17	1.57	2.55
38087	1.34	1.56	3.44
41094	1.25	1.67	2.67
41095	1.34	2.80	4.00
42099	1.27	1.67	2.53
44099	1.18	1.54	2.10
45105	1.52	1.62	4.40
46107	1.19	1.75	2.42
48111	1.24	1.80	2.61
49113	1.44	1.87	2.50
49115	1.47	1.93	2.90
50115	1.30	2.01	3.43
50116	1.13	1.63	2.38
50117	1.33	2.29	3.78
50118	1.06	1.57	2.16

ZA	d_1(%)	d_2(%)	χ_v^2
50119	1.12	1.62	2.48
50123	1.20	1.59	2.60
50126	1.17	1.59	2.74
51124	1.74	2.18	3.61
51125	1.31	1.73	2.38
52123	1.30	1.61	2.04
52124	1.07	1.80	2.29
52125	1.15	1.68	2.27
52128	1.10	1.69	2.37
53129	1.11	1.73	2.46
53131	1.32	1.97	2.87
54128	1.09	1.54	2.15
54129	1.20	1.75	2.31
54135	1.22	1.89	2.99
55134	1.35	2.14	2.89
55135	1.20	1.88	3.15
55136	1.29	2.19	3.89
55137	1.22	1.77	3.40
56130	1.32	2.02	2.40
56132	1.20	2.17	2.58
56135	1.20	1.81	2.54
56136	1.12	1.75	2.53
56137	1.12	1.98	2.49
57138	1.35	2.12	3.09
58140	1.21	1.73	2.70
58144	1.16	2.05	3.01
59143	1.17	1.61	2.79
61147	1.47	2.47	3.72
61148	2.23	3.25	6.13
61149	1.89	2.21	3.56
63152	2.43	3.56	4.32
63154	2.00	1.67	2.14
63156	1.53	1.85	3.08
65159	1.59	2.49	3.81
71175	1.79	1.55	4.27
71176	1.98	1.82	4.18
73182	1.47	1.65	2.63
80198	1.25	1.77	3.26
80199	1.60	2.89	5.87
80201	1.45	2.57	5.02
91230	1.81	1.60	6.44
91231	1.69	2.23	4.10
91232	1.76	1.55	5.84
92231	1.88	1.65	7.53
92233	2.71	3.55	52.0
93234	1.92	1.68	9.17
93236	2.22	1.76	9.75
93238	2.04	1.64	8.12
94236	1.91	1.75	9.16
94237	1.89	1.63	9.17
94238	1.92	1.61	3.66
95240	1.78	1.65	9.29
95242	2.08	1.83	18.5
96241	1.88	1.64	9.18
96242	1.40	2.06	6.96
96243	3.08	3.57	62.7
96244	1.29	1.65	3.80

ZA	$d_1(\%)$	$d_2(\%)$	χ_v^2
96245	2.80	3.66	72.4
96247	1.81	1.56	7.60
96249	1.51	1.52	8.41
97246	2.07	1.66	9.04
97248	1.93	1.69	9.50
98249	1.72	1.65	10.2
98251	1.49	1.53	7.85
98253	1.91	1.53	9.74
99252	2.22	1.78	13.8
99254	2.01	1.70	11.2
100255	2.21	1.82	13.1

TABLE 6. Nuclei from ENDF/B-VII.1 with $\chi_v^2 > 2$ and $d_2 > 1.5$, together with d_1, d_2 and χ_v^2.

ZA	$d_1(\%)$	$d_2(\%)$	χ_v^2
4007	5.99	-	33.2
26057	2.28	3.96	23.3
35081	1.17	1.57	2.55
38087	1.34	1.56	3.44
41094	1.25	1.67	2.67
41095	1.34	2.80	4.00
42099	1.26	1.68	2.53
44099	1.18	1.54	2.10
44106	1.07	1.50	2.16
46107	1.19	1.75	2.42
48111	1.24	1.80	2.61
49113	1.44	1.87	2.50
49115	1.47	1.93	2.90
50115	1.30	2.01	3.43
50116	1.13	1.64	2.38
50117	1.33	2.29	3.78
50118	1.06	1.57	2.15
50119	1.12	1.62	2.48
50123	1.20	1.59	2.60
50126	1.17	1.58	2.72
51124	1.76	2.32	3.72
51125	1.31	1.73	2.38
52123	1.30	1.61	2.04
52124	1.07	1.80	2.30
52125	1.15	1.68	2.27
52128	1.10	1.69	2.38
53129	1.11	1.73	2.46
53131	1.32	1.97	2.87
54128	1.09	1.54	2.15
54129	1.20	1.75	2.31
54135	1.22	1.89	2.99
55134	1.35	2.14	2.89
55135	1.19	1.88	3.15
55136	1.29	2.19	3.89
55137	1.22	1.77	3.40
56130	1.32	2.02	2.39
56132	1.20	2.17	2.58
56135	1.20	1.81	2.54
56136	1.12	1.75	2.53
56137	1.12	1.98	2.49
57138	1.35	2.12	3.09

ZA	$d_1(\%)$	$d_2(\%)$	χ_v^2
58140	1.21	1.73	2.70
58144	1.16	2.05	3.01
59143	1.17	1.61	2.79
61147	1.47	2.47	3.72
61148	2.23	3.25	6.12
61149	1.89	2.21	3.56
63152	2.43	3.56	4.33
63154	2.02	1.65	2.16
63156	1.53	1.85	3.08
65159	1.59	2.49	3.81
71175	1.79	1.55	4.27
71176	1.98	1.82	4.18
72174	1.30	2.07	2.66
72176	1.37	1.97	2.70
72177	1.80	2.80	4.01
72178	1.46	1.87	2.90
72179	1.58	2.67	3.87
72180	1.11	1.56	2.48
73182	1.47	1.65	2.63
80198	1.25	1.77	3.26
80199	1.60	2.89	5.86
80201	1.45	2.57	5.02
91230	1.81	1.60	6.44
91231	1.69	2.23	4.10
91232	1.76	1.55	5.85
92231	1.88	1.65	7.53
93234	1.92	1.68	9.17
93236	2.01	1.56	7.35
93238	1.85	1.59	7.12
94236	1.91	1.75	9.16
94237	1.89	1.63	9.17
94238	1.88	1.61	3.65
95240	1.78	1.65	9.29
95241	2.15	2.49	7.48
95243	1.93	2.28	5.64
96241	1.96	1.65	9.79
96242	1.53	2.09	7.59
96243	3.13	3.63	63.4
96244	1.50	1.53	3.33
96245	2.87	3.70	72.8
96247	1.72	1.52	8.01
96249	1.46	1.54	7.35
97246	1.98	1.61	8.49
97248	2.14	1.69	9.57
98249	1.63	1.64	9.64
98251	1.64	1.55	7.98
98253	1.88	1.56	9.16
99252	2.19	1.78	13.6
99254	2.27	1.74	12.0
100255	2.10	1.73	12.6

TABLE 7. Nuclei from BROND-3.1 with $\chi_v^2 > 2$ and $d_2 > 1.5$, together with d_1, d_2 and χ_v^2.

ZA	$d_1(\%)$	$d_2(\%)$	χ_v^2
4009	3.21	2.50	31.8
8018	4.08	4.48	94.7
26057	2.46	4.09	23.4
35081	1.17	1.57	2.54
38087	1.34	1.54	3.43
41094	1.25	1.66	2.66
41095	1.35	2.80	4.01
42099	1.27	1.66	2.53
44099	1.18	1.54	2.10
46107	1.18	1.74	2.41
49113	1.44	1.87	2.50
49115	1.48	1.93	2.90
50115	1.29	2.02	3.43
50116	1.13	1.61	2.36
50117	1.34	2.30	3.79
50118	1.06	1.56	2.15
50119	1.12	1.62	2.48
50123	1.20	1.59	2.59
50126	1.16	1.59	2.72
51124	1.76	2.31	3.71
51125	1.31	1.73	2.38
52123	1.30	1.61	2.03
52124	1.07	1.80	2.28
52125	1.15	1.69	2.27
52128	1.10	1.69	2.40
53129	1.11	1.73	2.46
53131	1.32	1.96	2.88
54128	1.09	1.53	2.14
54129	1.20	1.75	2.29
54135	1.22	1.89	3.00
55134	1.35	2.14	2.89
55135	1.20	1.88	3.15
55136	1.29	2.19	3.89
55137	1.22	1.76	3.39
56130	1.33	2.02	2.41
56132	1.20	2.18	2.58
56135	1.20	1.81	2.54
56136	1.11	1.73	2.51
56137	1.13	1.98	2.50
58140	1.21	1.74	2.70
58144	1.16	2.06	3.02
59143	1.18	1.61	2.80
61147	1.47	2.47	3.73
61148	2.23	3.26	6.13
61149	2.28	2.82	4.07
63152	2.43	3.56	4.32
63154	2.01	1.65	2.16
63156	1.53	1.85	3.08
65159	1.59	2.49	3.82
71175	1.78	1.54	4.26
71176	1.98	1.82	4.17
73182	1.48	1.65	2.63
90231	14.40	2.63	20.8
91233	6.96	14.05	134

ZA	d_1(%)	d_2(%)	χ^2_v
93236	3.70	1.57	8.59
93238	1.89	1.64	7.28
94237	1.72	1.69	9.11
94242	1.64	2.21	4.63
95241	1.96	2.49	6.81
95243	1.94	2.19	5.67
96243	2.73	3.54	122
96244	1.55	2.70	11.5
96245	2.91	4.32	37.6
96249	1.62	1.53	5.90

TABLE 8. Nuclei from JENDL-4.0U with $\chi^2_v > 2$ and $d_2 > 1.5$, together with d_1, d_2 and χ^2_v.

ZA	d_1(%)	d_2(%)	χ^2_v
43099	1.36	1.67	2.43
44101	1.25	1.60	2.43
44103	1.27	1.83	2.64
44099	1.15	1.52	2.08
45103	1.64	1.75	2.88
45105	1.94	1.54	7.24
51124	1.73	2.17	3.58
51125	1.28	1.66	2.20
52123	1.35	1.81	2.21
52125	1.13	1.67	2.17
52130	1.11	1.65	2.33
53127	1.30	2.20	2.99
53129	1.18	1.91	2.60
53131	1.33	1.98	2.92
56130	1.20	1.83	2.26
56132	1.20	1.92	2.46
56134	1.08	1.69	2.08
56135	1.20	1.93	2.60
56136	1.14	1.65	2.43
56137	1.05	1.60	2.19
56138	1.20	1.69	3.30
57138	1.38	2.08	3.02
57139	1.12	1.66	2.70
59141	1.40	2.00	4.04
59143	1.25	1.53	3.02
73181	1.32	1.61	2.15
80199	1.36	2.13	3.48
80201	1.24	2.05	3.56
91230	1.82	1.59	6.43
91232	1.76	1.56	5.94
92231	1.85	1.65	7.46
92233	2.65	3.68	56.0
92235	3.91	3.57	57.6
93234	1.94	1.69	9.23
93236	1.95	1.56	7.33
93238	1.82	1.61	7.13
94236	1.91	1.75	9.14
94237	1.91	1.61	9.09
94239	2.42	3.40	44.2
94241	1.79	1.58	7.52
95240	1.76	1.64	9.30

ZA	$d_1(\%)$	$d_2(\%)$	χ^2_v
95242	3.01	3.72	68.7
95244	1.73	1.57	6.69
96241	1.95	1.65	9.80
96242	1.53	2.10	7.59
96243	3.14	3.65	64.1
96244	1.51	1.51	3.26
96245	2.86	3.69	72.7
96247	1.70	1.52	7.96
96249	1.46	1.52	7.36
97246	1.97	1.61	8.51
97248	2.13	1.69	9.54
98249	1.68	1.64	9.61
98251	1.66	1.54	7.91
98253	1.87	1.59	9.25
99252	2.23	1.80	13.7
99254	2.30	1.73	12.1
100255	2.14	1.76	12.8

[1] The PHP_AS_HP flag

At compilation time it is possible to define the following flag in Geant4: PHP_AS_HP. If this flag is defined then the sampling procedure to generate secondary particles will be slightly different (see 0). We have performed the same test described in the previous section with and without defining this flag, using the JEFF-3.3 library. The obtained results are presented in Fig. 11, showing that according to this test the default behaviour is closer to MCNP6. Note that this does not mean that the results are closer to MCNP6 for every situation.

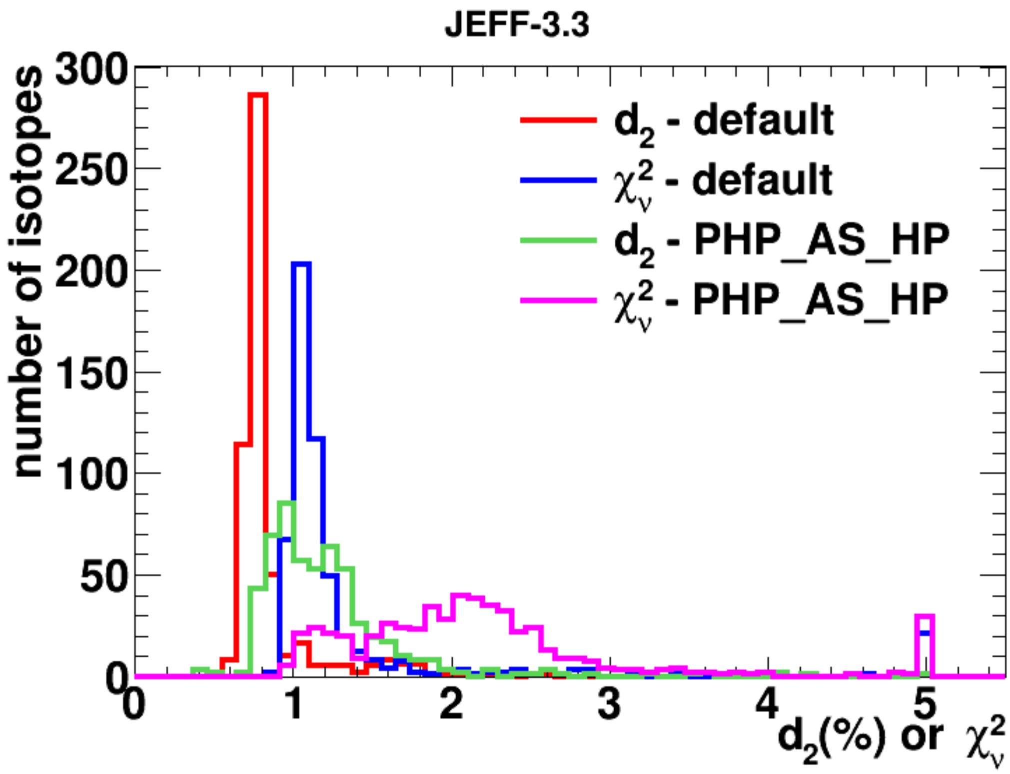

FIG. 11. Values of d_2 and χ^2_v obtained using JEFF-3.3 with the default Geant4 compilation ("default") and with a compilation performed with the option PHP_AS_HP turned on ("PHP_AS_HP").

5. SUMMARY AND CONCLUSIONS

The list of G4NDL libraries distributed by the IAEA Nuclear Data Services has been updated with six new releases: JEFF-3.3, JEFF-3.2, ENDF/B-VIII.0, ENDF/B-VII.1, BROND-3.1 and JENDL-4.0u (version 2016/1/6).

A comparison between Geant4 and MCNP6 when using these six new releases has been performed concerning the neutron transport. The differences between the obtained results have been quantified, showing a reasonable agreement between both codes and assuring the integrity of the converted libraries. Those isotopes showing larger discrepancies have been listed, together with the parameter values defining these discrepancies.

A large set of plots containing energy distributions obtained from Geant4 and MCNP6 simulations of the secondary neutrons, γ-rays, p, d, t, ^{3}He and α have been generated and are available from the IAEA Nuclear Data Services together with the libraries.

6. REFERENCES

[1] S. Agostinelli, *et al.*, Nucl. Instrum. Methods A **506** (2003) 250.

[2] Document ENDF-102, ENDF-6 Formats Manual: Data formats and procedures for the Evaluated Nuclear Data Files ENDF/B-VI, ENDF/B-VII and ENDF/B-VIII, BNL-203218-2018-INRE, M. Herman and A. Trkov (Eds), 2018.

[3] E. Mendoza, *et al.*, IEEE Trans. Nucl. Science **61** (2014) 2357.

[4] IAEA Nuclear Data Services, https://www-nds.iaea.org/geant4/.

[5] OECD/NEA Data Bank, JEFF-3.3 Nuclear Data library (2017), https://www.oecd-nea.org/dbdata/JEFF33/

[6] OECD/NEA Data Bank, JEFF-3.2 evaluated data library – Neutron data (2014), https://www.oecd-nea.org/dbforms/data/eva/evatapes/jeff_32/.

[7] D.A. Brown, *et al.*, Nucl. Data Sheets **148** (2018) 1.

[8] M.B. Chadwick, *et al.*, Nucl. Data Sheets **112** (2011) 2887.

[9] A.I. Blokhin, *et al.*, New version of neutron evaluated data library BROND-3.1, Yad. Reak. Konst. **2** (2016) 62.

[10] K. Shibata, *et al.*, J. Nucl. Sci. Technol. **48** (2011) 1.

[11] Summary of JENDL-4.0 updated files until 2016/ 1/ 6 (2016), http://wwwndc.jaea.go.jp/jendl/j40/update/update.php?date=20160106.

[12] D.E. Cullen, PREPRO 2017 - 2017 ENDF/B Pre-processing Codes ((ENDF/B-VII or Proposed VIII Tested), Technical report IAEA-NDS-39 (Rev.17), International Atomic Energy Agency, Vienna, Austria (2017).

[13] JAEA nuclear data center, http://wwwndc.jaea.go.jp/jendl/j40/update/.

The Geant4 collaboration, Book for application developers (release 10.4), available at http://geant4.cern.ch/support/userdocuments.shtml.